Article

Mechanism of Cesium Adsorption by Carbonized Rice Hull and Beech Sawdust

Asa Miura

University of Fukui, 3-9-1 Bunkyo, Fukui 910-8507, Japan; amiura@u-fukui.ac.jp; Tel.: +81-776-27-8695

check for
updates

Abstract: This study used the results of breakthrough experiments to elucidate the mechanism of cesium adsorption on carbonized rice hull and beech sawdust. The shape of the breakthrough curves and the substance eluted from the carbonized rice hull and beech sawdust were investigated for various flow speeds and concentrations of the solute through the adsorbent layer. The ratio of the Cs concentration at the column outlet (C) to that at the inlet (C_0), C/C_0, was calculated to evaluate the mechanism. It was found that carbonized rice hull could slowly adsorb Cs as the Cs solution passed through the fixed-bed layer. On the other hand, beech sawdust could rapidly adsorb Cs upon contact with the Cs solution. It was, therefore, suggested that the two materials adsorbed Cs through an ion-exchange reaction with potassium on their respective surfaces. Moreover, the shape of the breakthrough curve of beech sawdust changed as the Cs concentration at the column inlet was varied. This phenomenon was presumably caused by a factor other than the swelling or contraction of the adsorption layer. Further analysis revealed that the breakthrough curve of beech sawdust is indicative of an overshoot phenomenon when cesium was adsorbed by beech sawdust.

1. Introduction

Radioactive material leaking from the Fukushima Daiichi Nuclear Power Plant in the aftermath of The Great East Japan Earthquake (the 2011 Tōhoku earthquake) caused widespread damage to the surrounding environment. Six years after the accident, reconstruction activities are now being carried out in the area [1].

A large amount of radioactive material was deposited mainly in the deciduous broad-leaved forests [2] that occupy 70% of the land in Fukushima prefecture [3]. Moreover, brief periods of rain increased the dissolution of radioactive cesium in nearby streams [4]. These radioactive materials were then transported to the river system or remained as sediment in the riverbed, which then traveled to water bodies at lower altitudes, such as ponds or dammed lakes [5]. The cesium diffused into the water system, and the resulting concentration was low in a widespread area.

Measures to remove the diffused cesium from the environment began immediately after the accident. In particular, decontamination technology using zeolite and Prussian blue was employed in highly contaminated areas around the power plant [6–8]. However, in the widespread areas with a low concentration of contaminants in the water system, such as forests and agricultural land, inexpensive and manageable adsorption materials are considered more suitable for decontamination.

In the study presented here, the author examined natural materials utilized for the removal of cesium from environmental water. In a series of experiments, carbonized rice hull and beech sawdust were found to be natural materials with the ability to adsorb Cs. These natural materials can be reduced in volume by incineration after Cs adsorption, which facilitates effective processing. According to the author's previous report [9], the adsorption efficiency of carbonized rice hull was 80%–90% of the initial Cs concentration, and that of beech sawdust was around 50% of the initial Cs concentration. The

adsorption isotherm curves of both materials could be fitted to the Freundlich adsorption isotherm model. On the other hand, the breakthrough experiments using a glass column did not yield standard breakthrough curves [10] of Cs adsorption on these materials. Hence, both breakthrough curves did not fit a theoretical model [11,12].

Based on the author's previous study [10], it was presumed that the breakthrough curves of both carbonized rice hull and beech sawdust arise from adsorption mechanisms which are different from that represented by a normal breakthrough curve. If a breakthrough experiment is based on Cs adsorption on a fixed layer, it would be necessary to understand the adsorption mechanism of Cs in water. Therefore, the goal of this study is to experimentally elucidate the mechanism of Cs adsorption on carbonized rice hull and beech sawdust.

2. Materials and Methods

2.1. Materials

Two kinds of natural materials with grain shapes, namely, carbonized rice hull and beech sawdust, were used. Scanning electron microscopy (SEM, S-3400N, HITACHI Corp., Tokyo, Japan) images illustrating the surface morphology of the materials are shown in Figure 1. The materials have porous structures. Their specific surface areas (*A*; the surface areas of the masses of the material particles), bulk density, and pH in solution are listed in Table 1. The specific surface area was obtained using a krypton gas adsorption apparatus (BELSORP-28SA-SP, MicrotracBEL Corp., Osaka, Japan). The particle size distributions of both materials are shown in Figure 2; on average, the materials have particle sizes of 1~2 mm and exhibit similar particle distributions. The materials were dried at 60 °C for 24 h using a constant-temperature unit before testing and were then directly used for the tests without sifting, to avoid further processing conditions as much as possible so as to facilitate the materials' use in practical applications.

(**a**)   (**b**)
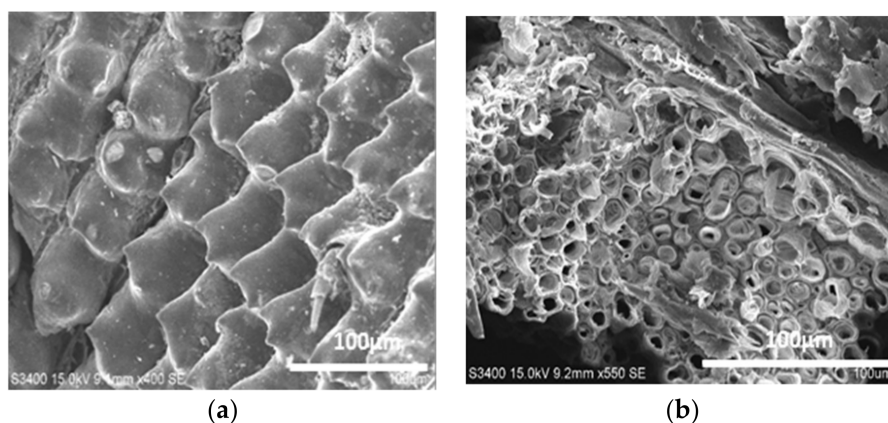
Figure 1. SEM images illustrating the surface morphology of the natural materials used in this study; (**a**) carbonized rice hull and (**b**) beech sawdust.

Table 1. Information for carbonized rice hull and beech sawdust.

Information for Materials	Carbonized Rice Hull	Beech Sawdust
Specific surface area; A (m^2 g^{-1})	3.4	0.35
Bulk density (g L^{-1})	122.6	211.7
pH in solution	7.25	3.42
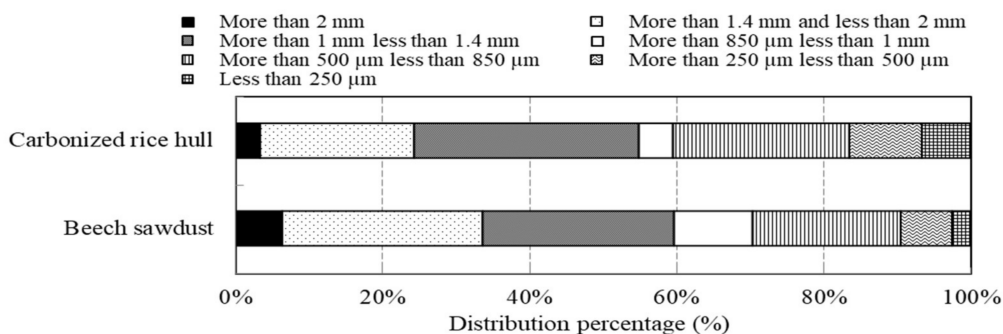
Figure 2. Particle size distribution of carbonized rice hull and beech sawdust.

2.2. Fixed-Bed Adsorption Experiments

The fixed-bed adsorption experiments were conducted using a glass column (height: 50 cm, diameter: 2 cm) with a continuous system. A schematic of the apparatus is shown in Figure 3; the experimental conditions are outlined in Table 2. The adsorbent was repeatedly packed without pressure in the column supported by sterile gauze at the bottom. The remaining space within the column not occupied by the adsorbent was filled with a degas solution. The solution was passed through a peristaltic pump (Cole-Parmer, Vernon Hills, IL, USA, MasterFlex L/S Series, Digital Pump Drives, easy-road Model 77202-60) to maintain the hydrostatic head above the column. The experiments were performed at a constant temperature of 25 °C.
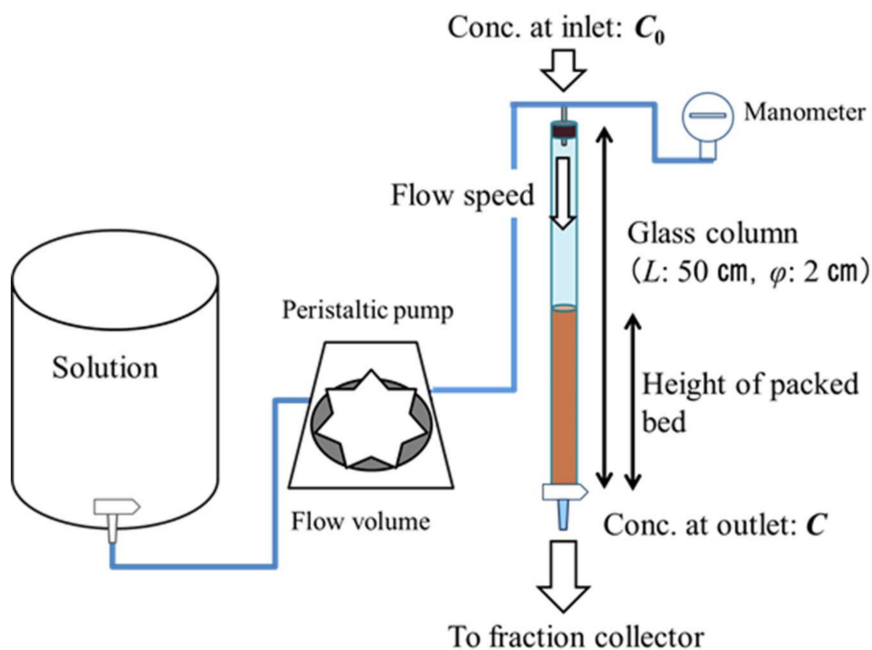
Figure 3. Schematic of the apparatus used in the fixed-bed adsorption experiments.

Table 2. Conditions at the breakthrough point and end point in experiment 1; (a) carbonized rice hull and (b) beech sawdust.

(a) Carbonized Rice Hull	Filled Adsorbent (g)	Height of Fixed Adsorbent Bed (cm)	Solution Flow Speed (mL min^{-1})	Cs Concentration (mg-Cs L^{-1})
C-1			5	
C-2	10	17	20	10
C-3			40	
(b) Beech Sawdust	**Filled Adsorbent (g)**	**Height of Fixed Adsorbent Bed (cm)**	**Solution Flow Speed (mL min^{-1})**	**Cs Concentration (mg-Cs L^{-1})**
B-1			10	
B-2	20	26	20	10
B-3			40	

Experiment 1 was conducted to investigate the breakthrough curves for a CsCl$_2$ solution passing through the column at various flow speeds with the packed-bed height held constant (by keeping the weights of the material constant). More specifically, three differential Cs solution flow speeds were used for the 17-cm high column of carbonized rice hull and 26-cm high column of beech sawdust in the packed bed (Table 2). The concentrations of Cs and K ions in the sampling water obtained at the outlet of the column were measured, and the breakthrough curves were analyzed with the variation of the Cs and K concentrations in the solution over time.

Based on the results of experiment 1, additional conditions were considered in experiment 2 to determine the mechanism of Cs adsorption on beech sawdust. In experiment 2-1, the breakthrough curves were examined for three differential Cs solution concentrations (1, 10, and 20 mg L^{-1}). In experiment 2-2, the breakthrough experiment was performed with an exchangeable Ca base included in the CaCl$_2$ solution; Ca concentrations of 1 and 5 mg L^{-1} were used. In these experiments, the pressure in the column was also measured with a water manometer (KDM30, Krone Corp., Tokyo, Japan).

At the outlet of the column, the Cs solution which was flowing through the column was collected by an automatic fraction collector (DC-1500C, Tokyo Rikakikai Co., Ltd., Tokyo, Japan). The solution sampling was performed at regular intervals of time. The sample solutions were filtered through membrane filters (pore size: φ0.45 μm, Whatman Inc., Maidstone, UK), and the concentration of the solute ions in the filtrates was analyzed using an ion chromatograph (IC-2010, Tosoh, Tokyo, Japan). Additionally, prior to the adsorption experiments, a blank test was conducted on the membrane filter using ion-exchanged water, thus establishing that the membrane filter did not contribute to cesium adsorption.

3. Results and Discussion

3.1. Breakthrough Curves for Cs Solutions at Various Flow Speeds (Experiment 1)

Experiment 1 was conducted with the Cs solution flowing into the fixed adsorption layer in the column at various speeds. The results for carbonized rice hull and beech sawdust are shown in Figure 4. The y axis represents the ratio of the Cs concentration at the column outlet (C) to that at the column inlet (C_0), C/C_0. The x axis represents the elapsed time since the solution began flowing at various speeds through the column. The origin of the x axis is set at the moment C/C_0 reached 0.5, and the negative values indicate the time elapsed before $C/C_0 = 0.5$.
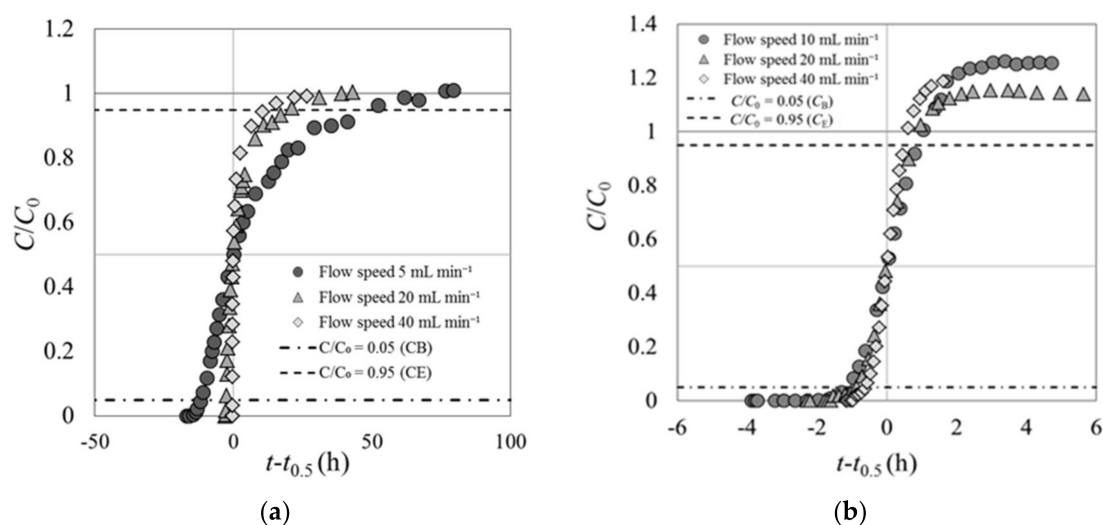
Figure 4. Breakthrough curves of (**a**) carbonized rice hull and (**b**) beech sawdust with the Cs solution flowing at various speeds (experiment 1).

Figure 4 shows C/C_0 (as well as C_B and C_E) at the breakthrough points (t_B) and end points (t_E) in the breakthrough curves of carbonized rice hull and beech sawdust. C_B is defined as the Cs concentration at the column outlet when C/C_0 reached 0.05, and C_E is the Cs concentration when C/C_0 reached 0.95. Table 3 shows t_B, t_E, and the elapsed time between t_B and t_E in the breakthrough curves of carbonized rice hull and beech sawdust.

Table 3. Elapsed time at the breakthrough point and end point in experiment 1.

Experiment 1	Carbonized Rice Hull			Beech Sawdust		
u: Flow speed of Cs solution (mL min^{-1})	5	20	40	10	20	40
t_B: Elapsed time at breakthrough point (h)	4.6	0.2	2×10^{-2}	2.5	1.4	0.5
t_E: Elapsed time at end point (h)	65.5	23.0	12.1	4.6	3.0	1.7
t_{B-E}: Elapsed time between C_B and C_E (h)	60.9	22.8	12.1	2.0	1.6	1.1

The shape of the breakthrough curves of each material remains constant regardless of the flow speed of the Cs solution passing through the column (Figure 4). These results are similar to those of previous breakthrough experiments on various fixed-bed adsorbent layers [10]. The trajectories of the breakthrough curves shown here are markedly different for different materials, and both curves deviated from the typical shape shown in published reports [13,14].

For carbonized rice hull, the breakthrough curves do not exhibit the typical S-shape with origin symmetry (Figure 4a). In experiment 1, the initial ratio of the Cs concentration at the column outlet increased rapidly until $C/C_0 = 0.5$, that is, the gradient of C/C_0 over the elapsed time was high. The last half of the curves exhibit lower gradients after C/C_0 reached 0.5. At the end point, the curves converge toward $C/C_0 = 1$ and reach flat plateaus. Moreover, the elapsed time from t_B to t_E was very long, namely 60.9 h at a Cs flow rate of 5 mL min^{-1}, 22.8 h at 20 mL min^{-1}, and 12.1 h at 40 mL min^{-1}.

On the other hand, the breakthrough curves of beech sawdust exhibit the standard S-shape (Figure 4b). However, the Cs concentration at the column outlet at the final stage exceeded the inlet concentration (overshoot) before reaching a flat plateau, that is, C/C_0 was about 1.2 times of unity. The feature characteristic of origin symmetry in these curves is different from that of the breakthrough curves of carbonized rice hull.

Based on these results, it is presumed that carbonized rice hull could not adsorb Cs immediately after it came into contact with the Cs solution, but started to slowly adsorb Cs as the Cs solution passed through the fixed-bed layer. On the contrary, beech sawdust could rapidly adsorb Cs immediately

upon contact with the Cs solution. However, this rapid adsorption was not long-lasting, because the Cs concentration at the outlet of the column exceeded the inlet Cs concentration within a short time.

Table 4 shows the Cs mass balance and the Cs adsorption rate in the time interval between t_E and t_B. Because the period between t_B and t_E, t_{B-E}, was very long for carbonized rice hull (Table 3), the total Cs inflow to the packed-bed layer was high and the amount of Cs remaining in it was increased (Table 4). On the other hand, t_{B-E} was relatively short for beech sawdust (Table 3), and both the Cs inflow and the amount of Cs remaining in the column were lower (Table 4). Therefore, the amount of adsorbed Cs was 4.5–7.5 mg per gram of carbonized rice hull and 0.3–0.7 mg per gram of beech sawdust (Table 4). However, after estimating the Cs adsorption ratio in the packed-bed layer during the period from t_E to t_B, it was found that 15.5%–36.6% of Cs was adsorbed by carbonized rice hull and 51.0%–55.6% of Cs was adsorbed by beech sawdust (Table 4). In other words, the amount of adsorbed Cs per gram of each material exhibited a trend that was opposite to that of the adsorption rate in the entire packed bed, presumably because of the difference in adsorption speeds of the materials.

Table 4. Cs mass balance in the packed-bed layer and Cs adsorption rate during experiment 1.

Experiment 1	Carbonized Rice Hull			Beech Sawdust		
Cs solution flow speed (mL min^{-1})	5	20	40	10	20	40
Total inflow of Cs (mg)	204.7	273.4	290.2	12.1	19.8	26.8
Total outflow of Cs (mg)	129.7	213.2	245.3	5.4	9.7	12.4
Total adsorbed Cs in column (mg)	75.0	60.2	44.9	6.7	10.1	14.4
Adsorbed Cs per unit weight of material (mg)	7.5	6.0	4.5	0.3	0.5	0.7
Cs adsorption rate in column (%)	36.6	22.0	15.5	55.6	51.0	53.6

In addition, the variation in the Cs flow speed was characterized by the amount of adsorbed Cs per gram of each natural adsorbent. The amount of Cs adsorbed by carbonized rice hull decreased when the Cs flow speed at the inlet of the column was increased (Table 4). On the other hand, the amount of Cs adsorbed by beech sawdust increased when the Cs flow speed was increased (Table 4). Although this is presumed to be related to the interaction between Cs and the materials' adsorption surface, the reason remains unclear.

In these breakthrough experiments on both materials, the K concentration eluted from each material varied in response to the variations in Cs concentration at the outlet of the column. The K concentration originally possessed by each material was measured by using an ammonium acetate solution. Each material and ammonium acetate solution were mixed at a ratio of 1:10 and shaken for 1 h, following which the K ions were extracted. The K ions eluted from carbonized rice hull and beech sawdust had concentrations of 1.86×10^4 mg L^{-1} and 1.7×10^4 mg L^{-1}, respectively, indicating that depending on the solute, it was possible to elute K from both materials. Figure 5 shows the relationship between the Cs and K ion concentration during the elapsed time between the breakpoint and the end point, t_{B-E}. These results show a strong negative correlation between the Cs and K ion concentrations for both carbonized rice hull and beech sawdust, with a correlation coefficient (R) of 0.99. Moreover, as shown in Figure 6, when ion exchange water was used instead of the Cs solution, the K ion concentration was relatively low throughout the experiment. Therefore, it can be concluded that Cs switched places with K through an ion-exchange reaction on the surface of each material.
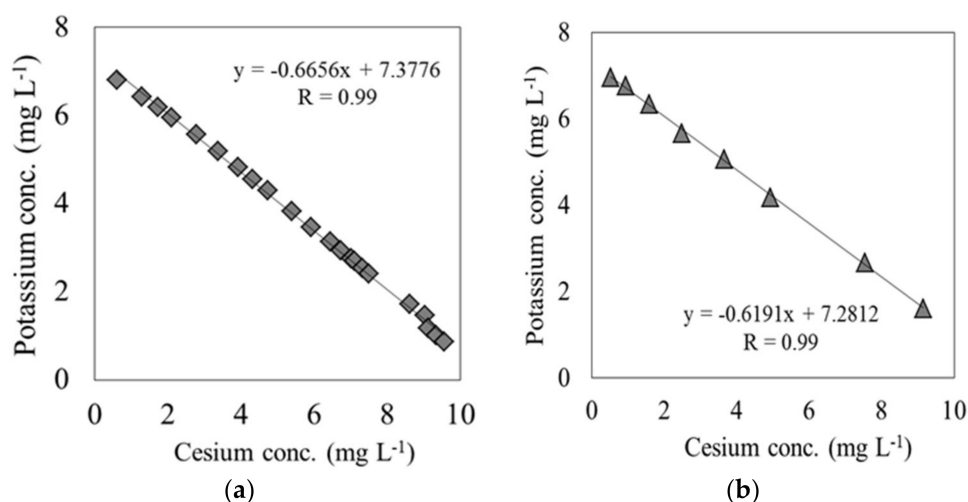
Figure 5. Correlation between the Cs concentration and K concentration at the outlet of the column: (**a**) carbonized rice hull; (**b**) beech sawdust (experiment 1).
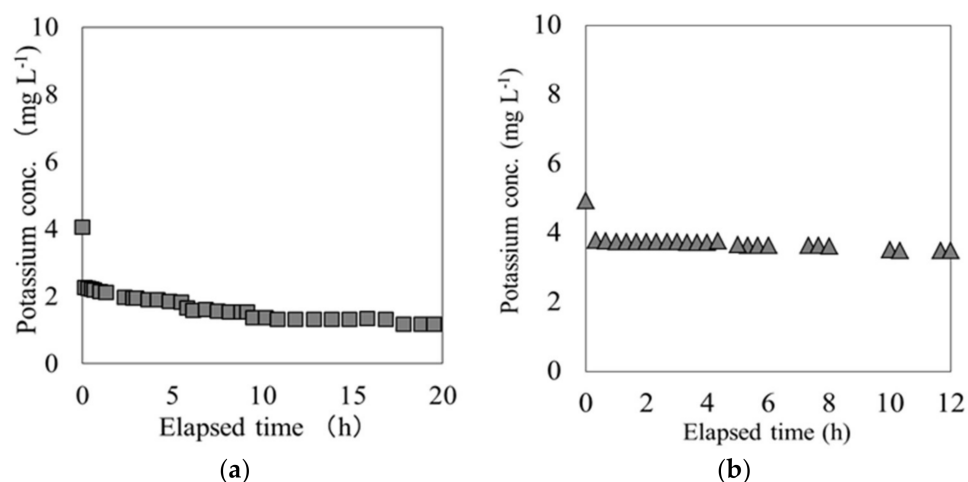
Figure 6. K elution from (**a**) carbonized rice hull and (**b**) beech sawdust in the breakthrough experiment.

3.2. Cs Adsorption by Beech Sawdust (Experiments 2-1 and 2-2)

The phenomenon of C/C_0 exceeding unity in the adsorption of Cs by beech sawdust in the breakthrough experiment was investigated through additional experiments.

First, experiment 2-1 was carried out to ascertain whether the Cs concentration at the outlet changed with respect to the Cs concentration in the solution at the inlet. Figure 7 shows the breakthrough curves for inflowing $CsCl_2$ solutions with Cs concentrations of 1, 10, and 20 mg L^{-1}. The *y* axis represents C/C_0, and the *x* axis indicates the elapsed time after the experiment began. It was found that incidences of $C/C_0 > 1$ (overshoot) increased as the Cs concentration was decreased in the solution at the inlet. When the solution had a Cs concentration of 1 mg L^{-1}, C/C_0 had a value of 2; when the Cs concentration was 20 mg L^{-1}, C/C_0 converged at 1 (without exceeding it). In these experiments, the pressure in the column was simultaneously measured, and was found to remain constant throughout. Had the pressure changed at the inlet of the column, the permeability coefficient of the adsorption layer would change, thereby implying that it would be possible for the adsorption layer to swell or contract. Therefore, the author believes that neither swelling nor contraction occurred in beech sawdust during Cs adsorption.
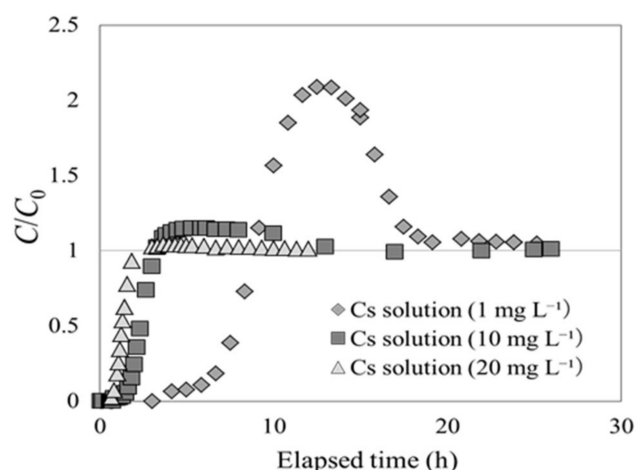
Figure 7. Cs adsorption breakthrough curves for beech sawdust, using Cs solutions with various Cs concentrations at the inlet (experiment 2-1).

As beech sawdust exhibited characteristic breakthrough curves in Cs adsorption, a solution containing a different solute was used to check if it would still exhibit the same phenomenon. In experiment 2-2, the breakthrough experiment was performed with an exchangeable base Ca included in the $CaCl_2$ solution. Ca concentrations of 1 and 5 mg L^{-1} were used in the $CaCl_2$ solution at the inlet of the column. The results of the experiment are shown in Figure 8. The shapes of the Ca adsorption breakthrough curves are similar to those of Cs adsorption for carbonized rice hull. Therefore, the phenomenon of C/C_0 exceeding unity before the equilibrium state may be a unique event for Cs and beech sawdust.
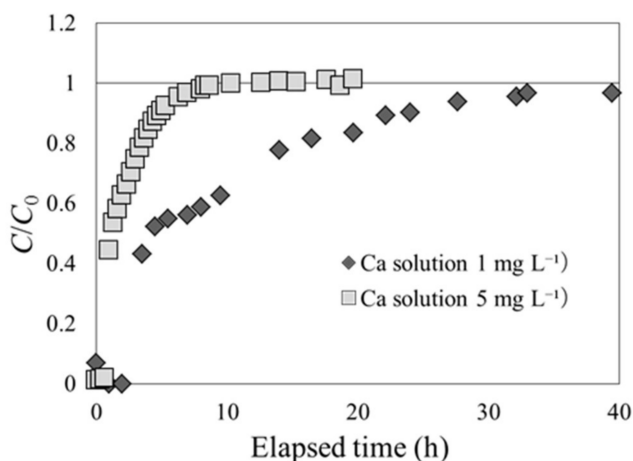
Figure 8. Ca adsorption breakthrough curves for beech sawdust, using Ca solutions with different Ca concentrations (experiment 2-2).

3.3. Overshoot in the Breakthrough Curve by Beech Sawdust

This section discusses the unique phenomenon observed in the breakthrough curve when beech sawdust adsorbs cesium.

In addition to the results of experiment 1 and experiment 2-1 obtained in this study, Table 5 lists the setting conditions and the values of C/C_0 in the breakthrough experiment using beech sawdust reported previously [10]. These breakthrough experiments were conducted under different conditions, in terms of the flow speed of the Cs solution, initial concentration of the C solution, and height of the packed bed of adsorbent in the column. Nevertheless, there was an overshoot when the maximum

outlet concentration (C) exceeded the column inlet concentration (C_0)($C/C_0 > 1$). There are several studies which report this overshoot phenomenon during the adsorption of various metals using adsorbents such as biomass-derived seaweed, activated sludge, and chelate resin [15–19]. Similar phenomena have also been reported in gas adsorption by activated carbon [20]. These studies attribute the origin of the phenomenon to bi-component systems. That is, during adsorption in a bi-component system, each component adsorbs competitively to the adsorption site in the initial stage; however, over time, one component attacks the adsorption site of another component. Thus, the overshoot phenomenon is qualitatively explained by the desorption of the other component. However, in this study, overshoot occurred for a mono-component (Cs). Therefore, in order to clarify this phenomenon exhibited by beech sawdust, it is necessary to carry out Cs adsorption experiments using beech sawdust under various experimental conditions.

Table 5. C/C_0 obtained from breakthrough curves of beech sawdust for adsorption under various experimental conditions.

Experimental Conditions (Beech Sawdust)	* Cs Solution Flow Speed (mL min^{-1})	C/C_0	* Initial Cs Concentration (mg-Cs L^{-1})	C/C_0	** Height of Fixed Adsorbent Bed (cm)	C/C_0
	10	1.3	1	2.1	15	1.1
	20	1.2	10	1.1	20	1.2
	40	1.2	20	1.0	26	1.2

* Results of this report; ** Results of the previous report (Miura, 2017).

4. Conclusions

Experiments were carried out in a column with a fixed adsorption layer to investigate the adsorption mechanism of carbonized rice hull and beech sawdust as natural adsorbents for the removal of Cs. On the basis of the results, the following conclusions can be drawn:

(1) The shape of the breakthrough curve of carbonized rice hull indicates that although it could not adsorb Cs immediately after contact with the Cs solution, it could slowly adsorb Cs as the Cs solution passed through the fixed-bed layer. On the contrary, beech sawdust could rapidly adsorb Cs immediately upon contact with the Cs solution.

(2) Cs switched places with K through an ion-exchange reaction on the adsorption surface of each material.

(3) The shape of the breakthrough curve of beech sawdust changed depending on the initial Cs concentration. As the Cs concentration at the column inlet was decreased, the value of C/C_0 markedly exceeded 1 (overshoot). However, there was no change in pressure in the column throughout the experiment, indicating that overshoot did not occur due to the contraction or swelling of the material in the column.

(4) Regardless of the experimental conditions for the breakthrough experiments, Cs adsorption by beech sawdust caused the overshoot phenomenon before reaching the equilibrium state.

Conflicts of Interest: The author declares no conflict of interest.

References

1. Fukushima Revitalization Station, Fukushima Prefecture Govt., Japan. Available online: http://www.pref. fukushima.lg.jp/site/portal/progress.html (accessed on 12 June 2017).
2. Hashimoto, S.; Ugawa, S.; Nakano, K.; Shichi, K. The total amounts of radioactively contaminated materials in forests in Fukushima, Japan. *Sci. Rep.* **2012**, *2*, 416. [CrossRef] [PubMed]
3. Kitamura, A.; Yamaguchi, M.; Kurikami, H.; Yui, M.; Onishi, Y. Predicting sediment and cesium-137 discharge from catchments in eastern Fukushima. *Anthropocene* **2014**, *5*, 22–31. [CrossRef]

4.   Iijima, K. Status of the researches on the behavior in the environment of radioactive cesium transported from forests to river systems. *Chikyukagaku* **2015**, *49*, 203–215. [CrossRef]

5.   Kurikami, H.; Kitamura, A.; Yokuda, S.T.; Onishi, Y. Sediment and ^{137}Cs behaviors in the Ogaki Dam Reservoir during a heavy rainfall event. *J. Environ. Radioact.* **2014**, *137*, 10–17. [CrossRef] [PubMed]

6.   Ishihara, R.; Fujiwara, K.; Harayama, T.; Okamura, Y.; Uchiyama, S.; Sugiyama, M.; Someya, T.; Amakai, W.; Umino, S.; Ono, T.; et al. Removal of cesium using cobalt-ferrocyanide-impregnated polymer-chain-grafted fibers. *J. Nucl. Sci. Technol.* **2011**, *48*, 1281–1284. [CrossRef]

7.   Saito, K. Removal of cesium from water using adsorptive fibers. *Bull. Soc. Sea Water Sci.* **2011**, *65*, 280–284.

8.   Shibata, J.; Furuyanaka, S.; Murayama, N.; Yoyogi, S. *Development of Processing Technology for Aqueous Liquor Containing High Level Radioactive Elements Discharged from Fukushima Nuclear Power Plant*; Disaster Prevention Research Institute, Kyoto University: Kyoto, Japan, 2012; pp. 1–20.

9.   Miura, A.; Kubota, T.; Hamada, K.; Hitomi, T. Adsorption efficiency of natural materials for low-concentration cesium in solution. *Water Sci. Technol.* **2016**, *73*, 2453–2460. [CrossRef] [PubMed]

10. Miura, A. Determination of cesium adsorption breakthrough curves using carbonized rice hull and beech sawdust as adsorbents. *Environ. Ecol. Res.* **2017**, *5*, 461–466. [CrossRef]

11. Michaelas, A.S. Simplified method of interpreting kinetic data in fixed bed ion exchange. *Ind. Eng. Chem.* **1952**, *44*, 1922–1930. [CrossRef]

12. Hashimoto, K. Design of fixed layer adsorption apparatus. *Water Purif. Liq. Wastes Treat.* **1972**, *13*, 37–47.

13. Vincent, C.; Hertz, A.; Vincent, T.; Barré, Y.; Guibal, E. Immobilization of inorganic ion-exchanger into biopolymer foams-Application to cesium sorption. *Chem. Eng. J.* **2014**, *236*, 202–211. [CrossRef]

14. Kim, T.Y.; An, S.S.; Shim, W.G.; Lee, J.W.; Cho, S.Y.; Kim, J.M. Adsorption and energetic heterogeneity properties of cesium ions on ion exchange resin. *J. Ind. Eng. Chem.* **2015**, *27*, 260–267. [CrossRef]

15. Kleinubing, S.J.; d'Silva, E.A.; d'Silva, M.G.C.; Guibal, E. Equilibrium of Cu (II) and Ni (II) biosorption by marine alga Sargassum filipendula in adynamic system: Competitiveness and selectivity. *Bioresour. Technol.* **2011**, *102*, 4610–4617. [CrossRef] [PubMed]

16. Figueira, M.M.; Volesky, B.; Climinelli, V.S.T.; Roddick, F.A. Biosorption of metals in brown seaweed biomass. *Water Res.* **2000**, *34*, 196–204. [CrossRef]

17. Naja, G.; Volesky, B. Multi-metal biosorption in a fixed-bed flow-through column. *Colloids Surfaces A Physicochem. Eng. Asp.* **2006**, *281*, 194–201. [CrossRef]

18. Sulaymon, A.H.; Yousif, S.A.; Al-Faize, M.M. Single-multicomponent biosorption of lead mercury chromium and arsenic onto activated sludge in batch and fixed-bed adsorber. *Desalin. Water Technol.* **2015**, *53*, 3499–3512. [CrossRef]

19. El-Sayed, M.M.H.; Chase, H.A. Simulation of the breakthrough curves for the adsorption of α-lactalbumin and β-lactoglobulin to SP Sepharose FF cation-exchanger. *Biochem. Eng. J.* **2010**, *49*, 221–228. [CrossRef]

20. Hori, H.; Tanaka, I.; Akiyama, T. A simple estimation method of breakthrough time for multicomponent organic solvent vapors on activated carbon fixed bed adsorbers. *Chem. Soc. Jpn.* **1985**, *11*, 2087–2093. [CrossRef]